

INSTRUMENTATION AND DATA-PROCESSING WORKFLOW FOR AMD NEUTRALIZATION: LINKING ROCK FORMATION, WATER-QUALITY MEASUREMENTS, AND INDEX COMPUTATION

Yazid Fanani^{1,3}, Eko Teguh Paripurno*¹, Tedy Agung Cahyadi², Ahmad Mushoffa³, Andris Emanuel Korompis³, M. Rizky Redy Asmara³, Dwi Fitri Yudwiantoro^{1,2}

¹Department of Geological Engineering, Universitas Pembangunan Nasional "Veteran", Yogyakarta, Indonesia ²Department of Mining Engineering, Universitas Pembangunan Nasional "Veteran", Yogyakarta, Indonesia ³Department of Mining Engineering, Institut Teknologi Adhi Tama Surabaya, Surabaya, Indonesia *paripurno@upnyk.ac.id

Received 2025-08-26, Revised 2025-10-24, Accepted 2025-10-28, Available Online 2025-10-28, Published Regularly October 2025

ABSTRACT

Acid mine drainage (AMD) forms when sulfide-bearing rocks react with oxygen and water, producing acidic, metal-rich discharges that threaten water quality. Addressing AMD requires a workflow that converts formation evidence and water quality data into operational treatment targets. This study applies the Integrated Geo-Hydrochemical Risk Assessment (IGHRA) as an instrumentation and data processing framework with three objectives: (i) to relate rock formation evidence to expected water quality behavior, (ii) to evaluate post treatment responses for quicklime (CaO) doses and limestone (CaCO₃) sizes under replicated bench tests, and (iii) to express treatment performance through diagnostic indices (CF, PLI) and compliance-based Residual Risk (RR). Methods include petrographic and bulk XRF for geochemistry analysis of eight rock samples, water quality measurements from nine stations, and bench experiments with five replicates per condition. Results show that CaO effectively restores pH to 6.0–6.4 and reduces Fe to 7–11 mg/L and Mn to 0.16 mg/L, while sulfate remains elevated (1.7 mg/L). Indices confirm risk reduction: PLI decreases from 3.18 to below 1.0 and RR from 66.67% to 16.67%. In contrast, CaCO3 treatments remain kinetically limited, with high indices across mesh sizes. To address residual solids, hydraulic residence time (HRT) analysis indicates that enlarging the polishing pond to 10,125 m³ provides 110 hours of detention time, compared to the current 9.6 hours. Overall, IGHRA translates posttreatment measurements into reproducible indices and design targets, providing a clear basis for AMD risk reduction.

Keywords: acid mine drainage; IGHRA; limestone; residual risk; quicklime.

INTRODUCTION

Acid mine drainage (AMD) is acidic, metal-rich water generated when sulfide-bearing rocks are exposed to oxygen and water during mining activities. This process harms water quality downstream and makes risk management more complex [1-3]. In practical terms, AMD lowers pH, mobilizes Fe and Mn, and generates conservative sulfate (SO₄), so solutions must translate measurements into operational decisions that are reproducible and auditable. Recent studies highlight the importance of connecting source characterization to risk reduction design. However, many researchers still examine hydrochemistry or valuation as separate issues. For instance, Gwira et al. (2024)^[4] measured health risks for mine waters but did not develop structured remediation strategies. Similarly, Czajkowski et al. (2023)^[5] assessed environmental

liabilities without linking them to a complete workflow from formation to water. To close this gap, we implement an Integrated Geo-Hydrochemical Risk Assessment (IGHRA). Here, IGHRA is used as a measurement and data processing workflow that links rock formation evidence, water quality measurements, and index computation to support dosing decisions and a polishing step. In this study we adopt an instrumentation perspective: we emphasize what is measured, how it is processed, and how the results set control targets for treatment.

Within IGHRA, we utilize two complementary sets of indicators ^[6,7]. First, contamination factors (CF), summarized as the Pollution Load Index (PLI), effectively detail Fe, Mn, SO₄ loads for spatial analysis. Second, a compliance oriented Residual Risk (RR) metric reports the number of regulatory limits of six parameters: pH, TDS, TSS, Fe, Mn, and SO₄ that exceed Class-IV benchmarks from Government Regulation (PP) No. 22/2021^[8] standards at each location. Both indicators are highlighted in recent guidelines and reviews ^[9-11] and are commonly applied to waters affected by mining ^[12-14]. Together, they maintain diagnostic sensitivity to AMD processes while being directly comparable to established standards. PLI provides a single diagnostic score from Fe, Mn, SO₄, whereas Residual Risk (RR) expresses compliance as the fraction of six parameters exceeding Class-IV thresholds.

This study creates a workflow for instrumentation and data processing that aims to (i) relate rockformation evidence to expected water quality behaviour; (ii) evaluate post treatment responses for quicklime (CaO) dose series and limestone (CaCO₃) size series under replicated bench tests; and (iii) express performance in diagnostic (CF, PLI) and compliance (RR) terms to set dosing and polishing targets. Evidence from formations helps identify sulfide sources and predict Fe, Mn, SO₄ behavior^[15-17]. Water sampling and analysis follow national methods^[18] and Class-IV benchmarks from Government Regulation (PP) No. 22/2021 define pass or fail thresholds used by the indices. For treatment, we use Ca-based alkalis, specifically quicklime (CaO) and limestone (CaCO₃), as the as the primary reagents. This is based on recent studies and reviews at mine scale ^[19-22]. This process quantifies dose to response effects on pH, Fe, Mn, and SO₄, monitors TSS polishing where necessary, and shows risk reduction using CF, PLI and RR that meet government standards. The polishing step is sized hydraulically using the residence time relation, where the hydraulic residence time (HRT) is obtained by dividing the effective pond volume and the inflow rate. This provides an operational envelope for solids removal and performance smoothing.

In Indonesia, AMD pollution represents both a technical challenge and a legal environmental obligation. Law No. 24/2007^[23] categorizes AMD related pollution as a non natural disaster, requiring rehabilitation, reconstruction, and socio economic recovery. Planning must fit within the framework of environmental governance. This includes Government Regulation (PP) No. 26/2025^[24] on environmental planning tools and Government Regulation (PP) No. 22/2021 on water quality standards, which form the basis for our CF, PLI and residual risk thresholds. Placing AMD control within this legal framework clarifies accountability and links measurement-based risk reduction to enforceable results.

METHOD

Study design and IGHRA-based workflow

We structure the study as an IGHRA (Integrated Geo-Hydrochemical Risk Assessment) to convert measurements into operational control. The workflow links three parts: (i) rockformation evidence from rock megascopic descriptions, rock petrographic analysis, and bulk XRF for geochemistry analysis to establish AMD potential and expected behaviour of Fe, Mn, and SO₄; (ii) replicated water quality measurements across the drainage to quantify post-

treatment responses; and (iii) index computation for contamination factors (CF) summarized as PLI (Fe, Mn, SO₄) and a compliance oriented Residual Risk (RR) over pH, TDS, TSS, Fe, Mn, SO₄ to express performance against Class-IV benchmarks from Government Regulation (PP) No. 22/2021. The indices then inform CaO dose set-points, while hydraulic residence time (HRT) defines the polishing envelope for solids control. Figure 1 summarizes this measurement and data processing workflow from formation to indices and control.

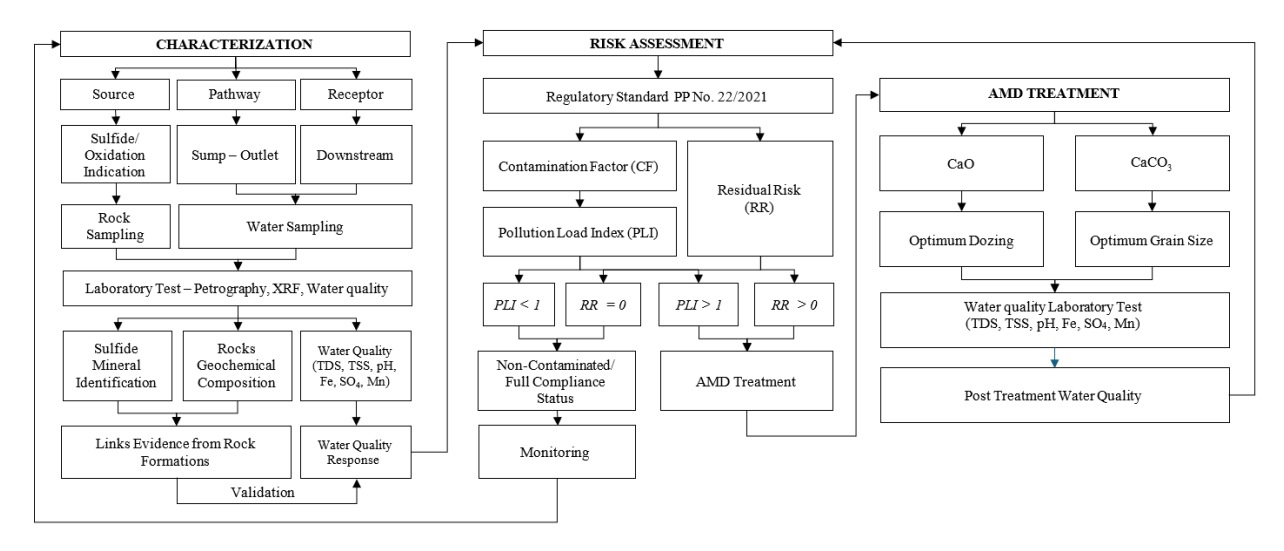


Figure 1. IGHRA instrumentation and data processing workflow.

Rock sampling and laboratory characterization

Hand specimen boulders were collected by dry grab from exposed pit faces across two benches with eight stations in total from pyrophyllite mining concession in South Malang, Indonesia. At each station, three to five pieces samples were prepared for petrographic and bulk XRF for geochemistry analysis. This bench distributed design follows the formation evidence parts of the IGHRA approach used in the pre treatment study, enabling bench scale comparison of lithology and alteration associated with sulfide occurrence.

Petrography quantifies modal percentages and textures such as opaque sulfides and sericitic alteration, while XRF uses dried, homogenized powders (≤200 mesh) prepared as pressed pellets or fused beads to determine major and trace elements with emphasis on Fe, S, and Mn as AMD source proxies. To minimize leverage from outliers, summary statistics are reported as median (IQR).

Water sampling and analytical methods

We sampled nine surface water stations (L1–L9) along the pit to receiving water transect. At each station, we composited surface and bottom grab samples into pre rinsed HDPE jerrycans, preserved them, transported them in accordance with relevant SNI/APHA field procedures as conditions allowed, and submitted them to the Surabaya City water-utility (PDAM) laboratory for analysis of pH, TDS, TSS, sulfate (SO₄), and dissolved iron (Fe) and manganese (Mn). Analysis followed the corresponding SNI/APHA methods.

Table 1 outlines the monitoring network and each station's function in the IGHRA workflow. Stations L1–L3 are classified as in-pit (source) and are used to characterize formation driven chemistry at the point of generation (sulfide oxidation context). Station L4 is the pond outlet (control/effluent) and serves as the post treatment control point where dose response outcomes and indices (PLI, RR) are assessed against Class-IV benchmarks from Government Regulation (PP) No. 22/2021. Stations L5–L9 are stream (downstream) locations that track the propagation

of AMD signatures and the effectiveness of risk reduction along the drainage. This layout anchors the measurement to decision workflow: source stations constrain the problem, the control point quantifies treatment performance, and downstream stations verify outcomes in receiving waters.

Table 1. Station metadata

Station ID	Station Type	Role in Workflow
L1	in-pit	source
L2	in-pit	source
L3	in-pit	source
L4	pond outlet	control/effluent
L5	stream	downstream
L6	stream	downstream
L7	stream	downstream
L8	stream	downstream
L9	stream	downstream

Table 2 lists the standards, instruments, and units used for all analytes in this study. pH was measured according to SNI 6989.11:2019 using a calibrated pH meter (unitless). TSS followed SNI 6989.3:2019 with a gravimetric determination (mg/L). TDS followed SNI 6989.27:2019 using gravimetric and conductivity approaches as specified (mg/L). Sulfate (SO₄) was analyzed by the turbidimetric method SNI 6989.20:2019 (mg/L). Dissolved Fe and dissolved Mn were determined under APHA 3120B (2017) using ICP-OES or atomic absorption (mg/L). All results are reported in mg/L except for pH. These national and APHA standards enable replication and cross study comparability.

Table 2. Analytical methods

Analyte	Method Code	Instrument	Units
pН	SNI 6989.11:2019	pH meter	-
TSS	SNI 6989.3:2019	Gravimetric	mg/L
TDS	SNI 6989.27:2019	Gravimetric/Conductivity	mg/L
SO_4	SNI 6989.20:2019	Turbidimetric	mg/L
Fe (dissolved)	APHA 3120B (2017)	ICP-OES/AA	mg/L
Mn (dissolved)	APHA 3120B (2017)	ICP-OES/AA	mg/L

Bench-scale treatment experiments

Reagents and sample handling. Raw mine-water was collected according to national sampling practice^[18] and preserved as required for subsequent analyses (where provided by the laboratory). Base reagents consisted of quicklime (CaO) and limestone (CaCO₃) supplied in particle size classes defined by the sieve mesh number. Reagents were stored dry and prepared immediately before dosing. All glassware and containers were cleaned and rinsed with deionized water; instruments were checked and calibrated per laboratory routine.

Experimental design. Two complementary series were performed with five replicates (n = 5) per condition: (i) CaO dose series to establish dose response behaviour for pH, Fe, Mn, and SO₄, and (ii) CaCO₃ size series at fixed mass to examine the sieve mesh number dependent response under identical bench conditions. The CaO series provides the operative control variable for treatment set points, whereas the CaCO₃ series is evaluated as a kinetics limited comparator at low pH. All analysis followed the methods and instruments listed in Table 2, and

compliance interpretation used Class-IV benchmarks from Government Regulation (PP) No. 22/2021 in Table 3.

Bench procedure. For each test unit, a measured volume of raw water was placed in a clean vessel. The assigned CaO dose (mass per volume) or CaCO₃ size class (fixed mass) was introduced and dispersed by controlled mixing to ensure homogeneous contact. After the prescribed contact and clarification sequence, supernatant aliquots were withdrawn from a consistent depth for analysis. Subsamples for dissolved metals (Fe and Mn) were filtered and acidified as required by APHA. pH, TSS, TDS, SO₄, Fe, and Mn were then determined using the standards in Table 2.

Data reduction. For each condition (dose or size by the sieve mesh number), replicated five times were summarized by the median and interquartile range (IQR). These summaries were used to construct the dose response (CaO) and size response (CaCO₃) figures in the Results. Post-treatment contamination factors from Fe, Mn, SO₄ were computed and summarized as PLI. Residual Risk (RR) was computed as the fraction of pH, TDS, TSS, Fe, Mn, and SO₄ exceeding Class-IV Government Regulation (PP) No. 22/2021 thresholds, as specified in Table 3

Analytical determinations follow SNI 6989.11:2019 (pH), SNI 6989.3:2019 (TSS), SNI 6989.27:2019 (TDS), SNI 6989.20:2019 (sulfate), and APHA 3120B (2017) (dissolved Fe and Mn). General laboratory practice, sampling, filtration, preservation, and quality control follow the relevant guidance in APHA Standard Methods where provided by Surabaya City water-utility (PDAM) laboratory.

Index computation and compliance thresholds

We use three complementary indices to translate post-treatment measurements into diagnostic and compliance terms. The Contamination Factor (CF) quantifies relative enrichment with respect to a reference or standard for each analyte following Håkanson, 1980 ^[6]. The Pollution Load Index (PLI) aggregates CF values into a single diagnostic score following Tomlinson et al., 1980^[7]. A compliance style Residual Risk (RR) expresses the fraction of regulated parameters that exceed Class-IV thresholds defined in Government Regulation (PP) No. 22/2021^[8], which provides a direct link to regulatory performance.

Indices are computed on post-treatment chemistry to express treatment performance:

• Contamination factors (CF) for Fe, Mn, and SO₄ were computed using PP No. 22/2021 Class-IV thresholds as reference concentrations, following Håkanson, 1980^[6]. In Equation (1), Ci denotes the measured concentration (mg/L), Si the applicable standard (Class-IV regulatory threshold), and i ∈{Fe,Mn,SO₄}. The quantity CFi is unitless and expresses concentration relative to the standard.

$$CF_{i} = \frac{C_{i}}{S_{i}} \tag{1}$$

• Pollution Load Index (PLI) as the geometric mean of contamination factors (CF), following Tomlinson et al., 1980^[7]. In Equation (2), CF₁, CF₂, ..., CF_n are the contamination factors for Fe, Mn, and SO₄, and n is the number of diagnostic parameters (here n=3). The index is unitless; by construction, PLI > 1 indicates an overall contaminated status and PLI < 1 indicates a non-contaminated (compliant) status.

$$PLI = (CF_1 \times CF_2 \times \dots \times CF_n)^{1/n}, \quad n = 3$$
(2)

• Residual risk (RR) is the percentage of the six regulatory parameters—pH, TDS, TSS, Fe, Mn, and SO₄—that exceed their Class-IV Government Regulation (PP) No. 22/2021^[8] limits at a given site and sampling event (compliance summary). RR ranges from 0% (full compliance) to 100% (all parameters exceed). If any parameter is missing, the percentage is calculated over the available parameters. Residual risk (RR) defined as:

$$RR(\%) = 100 \times \left(\frac{N_{\text{exceed}}}{N_{\text{total}}}\right) \tag{3}$$

The computation of indices requires regulatory thresholds as reference points. In this study, we use the Class-IV water quality standards defined in Government Regulation (PP) No. 22/2021 of Indonesia. These benchmarks specify the acceptable ranges or maximum limits for pH, TDS, TSS, Fe, Mn, and SO₄, and serve as the reference concentrations (Si) in Equation (1) for CF, the baseline for PLI, and the compliance thresholds for RR. Table 3 summarizes the values adopted in this study.

Parameter	Threshold Type	Value	Units
pН	range	6–9	-
TDS	max	2,000	mg/L
TSS	max	400	mg/L
Fe	max	10	mg/L
Mn	max	5	mg/L
SO4	max	400	mg/L

Table 3. Regulatory benchmarks used in this study

Polishing design method

Neutralization generates suspended solids that require an additional polishing step to achieve effluent compliance. To design this step, we apply the concept of hydraulic residence time (HRT) by dividing the effective pond volume (V) and the inflow rate (Q). Following Decree of the Minister of Energy and Mineral Resources (KEPMEN ESDM) No. 1827/2018^[28], a minimum detention time of 84 hours is adopted as the design limit. Internal hydraulic controls such as compartments and baffles are included to reduce short circuiting and enhance settling efficiency. Figure 2 illustrates the schematic configuration of the compartmental settling pond proposed in this study.

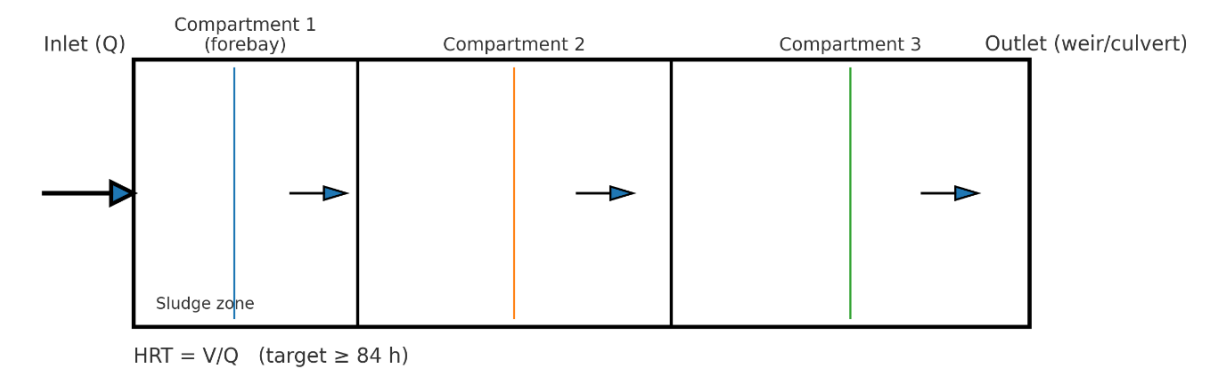


Figure 2. Compartmental settling-pond schematic

RESULTS AND DISCUSSION

Formation-hydrochemistry linkage

The petrographic observations provide a direct link between rock composition and the likelihood of generating acid mine drainage. Quartzolite and vitric tuffs, which dominate the samples, contain little natural buffering capacity but host opaque sulfides that can oxidize to release acidity. Phyllic-altered rhyolite and dacite further show sericitization and disseminated sulfides, marking zones of intense weathering and acid generation potential. These characteristics are summarized in Table 4, which lists the modal mineral percentages for each sample.

Table 4. Petrography summary

Sample	Lithology	Quartz (%)	Feldspar/ Plagioclase (%)	Opaque sulfides (pyrite) (%)	Vitric glass (%)	Sericite (%)
S1	Quartzolite	68	4	2		
S2	Vitric tuff	41		4	55	
S 3	Quartzolite (sulfide-rich)	48	3	24		
S4	Quartzolite	68	4	2		
S5	Alkali-feldspar rhyolite (phyllic- altered)			2		47
S 6	Vitric tuff	41		4	55	
S7	Dacite (phyllic- altered)	22		3		50
S 8	Quartzolite	68	4	2		

To complement the petrography, bulk geochemistry was determined by XRF, with emphasis on iron, sulfur, and manganese as primary proxies of acid generation and trace metals as secondary indicators. The results confirm high Fe and S concentrations in several samples (notably S3 and S7), consistent with abundant sulfide occurrence. Elevated Mn in S7 further emphasizes site-specific risks. These results are compiled in Table 5.

Table 5. Bulk XRF summary

Sample	Fe	Mn	S	Cu	Zn	Ni	Pb	Se
S 1	11,380	1.5	1,082	5.7	5.2	8.1	6.4	0.2
S2	9,322	5.7	5,240	103.3	10	13	2.8	15.5
S3	83,090	9.9	6,708	15.1	10.8	13.5	15.6	< 0.3
S4	11,371	1.6	1,084.7	5.7	4.9	7.8	7.1	0.1
S5	13,810	22.4	5,725	27.4	17	10.4	< 0.1	1.8
S 6	9,336	5.5	5,248.9	102.5	10	13.7	2.6	15.5
S 7	93,400	2,554	1,727	22	205.1	51.6	3.1	0.5
S8	11,369	1.5	1,082	5	4.5	7.8	6.2	0.3

Taken together, the petrographic and geochemical evidence indicates that the studied formations provide abundant sulfide sources but very limited buffering capacity, which explains the persistent acidity observed in drainage waters.

CaO dose-response

Bench tests with quicklime show a steady increase in pH with dose, moving from strongly acidic to neutral at the highest dose. This change is accompanied by significant drops in

dissolved Fe and Mn. Mechanically, CaO breaks down to Ca(OH)₂, which raises alkalinity. This process drives the hydrolysis and precipitation of Fe(III) oxyhydroxides. Fe(II) removal follows due to oxidation and subsequent precipitation. Mn removal happens at higher pH through Mn(OH)₂ and Mn-oxyhydroxides, and through co-precipitation and adsorption onto newly formed Fe flocs ^[25]. The median levels indicate that Fe decreases from 459 mg/L at 1 g/L to 9 mg/L at 10 g/L, while Mn drops from 0.23 mg/L to 0.16 mg/L over the same range. The interquartile ranges remain narrow across five replicates, showing consistent responses.

Sulfate (SO₄) shows only small decreases with dose, falling from about 5,600 mg/L at 1 g/L to 1,750 mg/L at 10 g/L, which is typical in neutralization systems. Minor declines result from dilution, ion pairing, and occasional gypsum formation when Ca is plentiful^[26]. However, stoichiometric limits and short bench contact times leave sulfate as the main factor for compliance. Total suspended solids (TSS) rise sharply after dosing due to floc generation, peaking at 724 mg/L at 4 g/L, and then stabilize to 155–188 mg/L at 7–10 g/L as settleable flocs dominate, which calls for a polishing step to ensure solids removal and maintain metal compliance. Total dissolved solids (TDS) decrease from 3,500 mg/L at 1 g/L to 1,725 mg/L at 10 g/L, reflecting the changing ionic strength, though still above the regulatory limit until sufficient dose or hydraulic residence time is applied.

In summary, the dose response shows that CaO is an effective neutralization agent for this matrix. It quickly restores pH and reduces Fe and Mn through solid formation while leaving sulfate, and to a lesser extent TDS and TSS, as the main residuals to manage downstream. The overall dose response behavior is summarized in Figure 3. The figure presents the median values with interquartile ranges across five replicates for each CaO dose, showing the systematic increase in pH, the strong decrease in Fe and Mn concentrations, and the limited changes in SO₄.

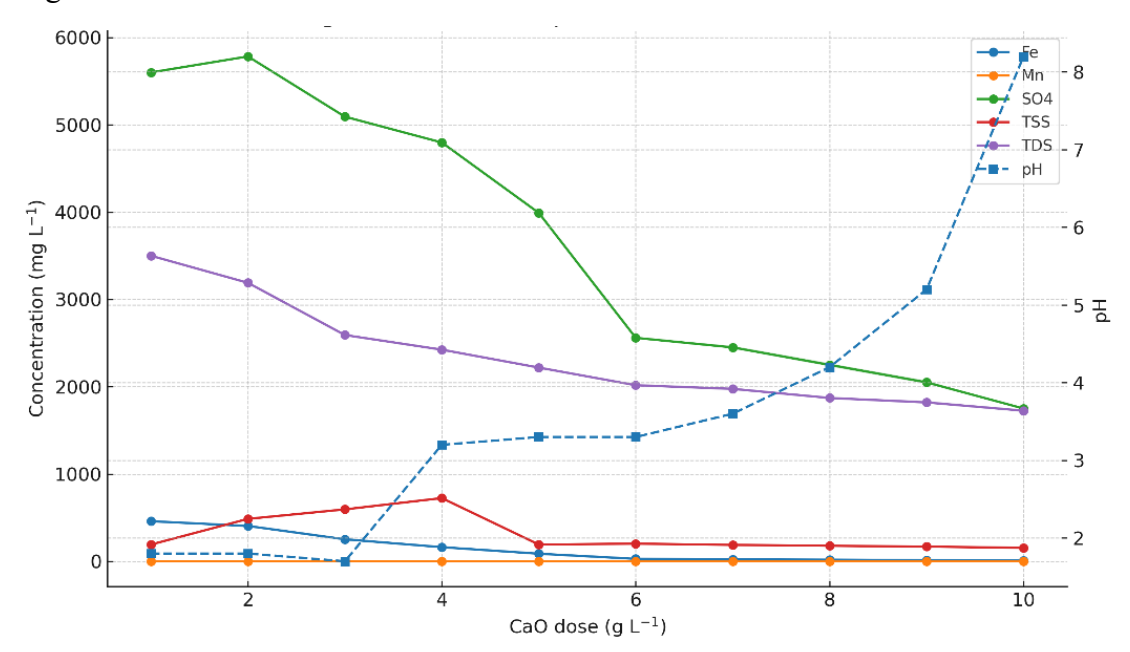


Figure 3. CaO dose-response; medians with IQR

CaCO₃ size-response

At a fixed dose, different limestone mesh mainly affects specific surface area and mass-transfer rates. However, under very acidic initial conditions, the system stays limited by reaction speed. Across five replicates per sieve mesh number sizes, the median pH stays very low, ranging only from 1.8–2.2 across sieve mesh number 10–60, well below the regulatory range of 6–9.

Dissolved Fe shows modest removal, with median values fluctuating around 350–500 mg/L, while Mn remains consistently low but non-compliant at 0.2–0.3 mg/L. Sulfate (SO4) concentrations dominate the response, staying extremely high between 4,600 and 19,500 mg/L, with the highest median value observed at sieve mesh number 4. These values clearly exceed the Class-IV limit of 400 mg/L, showing sulfate (SO4) as the controlling factor.

Finer fractions (mesh number 40–60) exhibit a slight benefit due to greater reactive surface area, with sulfate dropping closer to 4,000–4,600 mg/L compared to coarser sizes, but this remains far from compliance. This behavior supports carbonate dissolution theory^[27]. At low pH, the dissolution of calcite, promoted by protons, starts off quickly but is soon restricted by surface armoring from Fe oxyhydroxide films, boundary layer diffusion control, and CO₂–carbonate speciation. Without an external alkalinity boost, the system cannot reach the pH levels needed for effective Fe and Mn precipitation. As a result, CaCO₃ is not effective as the main neutralizing agent for this mix. Its practical use is as a polish, which essentially adds alkalinity after CaO-based neutralization, when the pH is already higher and the reaction speeds are favorable.

The comparative results for different CaCO₃ mesh sizes are shown in Figure 4. Each series represents the median values with IQR-based error bars across five replicates. The figure highlights the limited changes in pH, Fe, Mn, and SO₄ across sieve mesh number sizes, with only minor improvements for finer fractions due to greater reactive surface area.

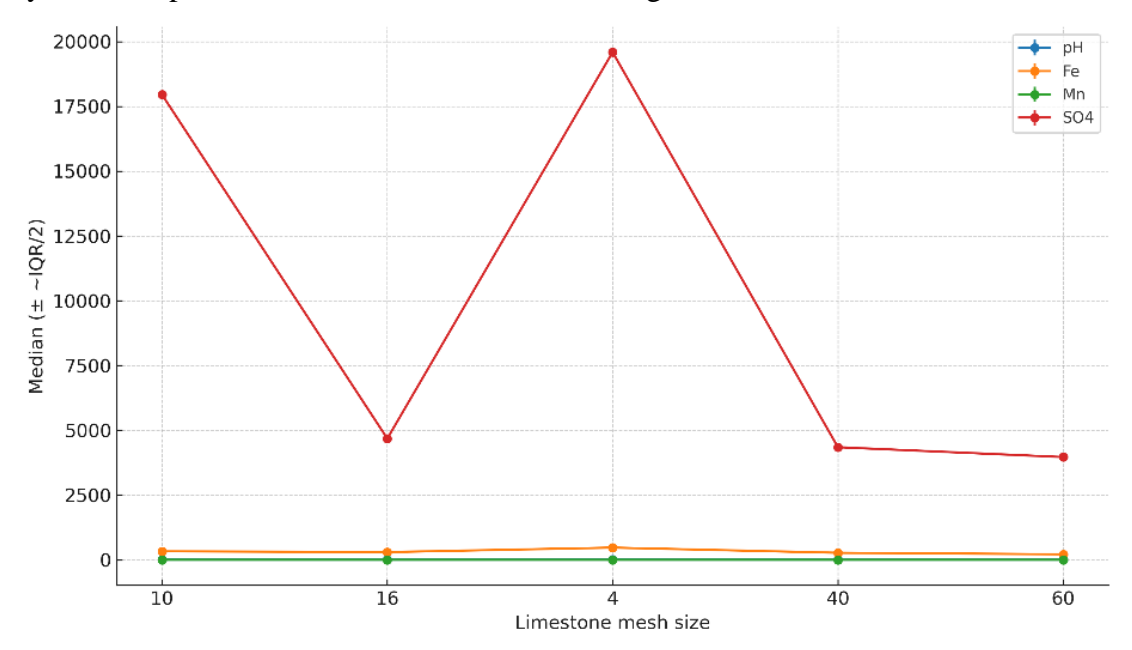


Figure 4. CaCO₃ size–response; medians with IQR-based error bars

Post-treatment diagnostic indices (CF-PLI) and compliance (RR)

We computed indices on post-treatment samples to show performance in diagnostic and compliance terms. For CaO, PLI (dose), which is the geometric mean of CF from Fe, Mn, SO₄, decreases with dose. The metal subset often reaches PLI < 1, while the total PLI > 1 when SO₄ is the dominant factor. Residual Risk (RR) also drops sharply with CaO, getting close to the lowest possible value with our analytic set. However, RR remains non-zero whenever SO₄ exceeds the Class-IV limit, as shown in the thresholds in Table 3.

For CaCO₃, indices calculated by mesh from post-treatment medians (n = 5 per sieve mesh number) stay high, with a PLI value between 2.2 and 4.9 and an RR value between 67 and

83%. The exceedances are mostly due to SO₄, along with Fe, TDS, low pH and TSS for finer fractions, reflecting the kinetic limits seen in Fig. 4. These differing trends indicate that (i) CaO is an effective neutralization agent in this context, and (ii) sulfate is the key factor controlling whether the overall index achieves compliance. Therefore, we present PLI(dose) and RR(dose) as control curves only for CaO, while treating limestone as a secondary post-neutralization alkalinity buffer rather than the main neutralization agent.

Table 6 summarizes the post-treatment diagnostic indices and compliance values for each CaO dose. The results show that contamination factors (CF) for Fe and Mn decline rapidly with increasing dose, while sulfate remains consistently high. Consequently, the PLI decreases from about 3.18 at 1 g/L to below 1.0 at doses of 6 g/L and above, although the overall PLI still reflects the persistent sulfate contribution. Residual Risk (RR) follows a similar pattern, falling from over 60% at low doses to about 16.67% at the highest dose, but never reaching zero because of the sulfate exceedance.

Dose	pН	TDS	TSS	Fe	Mn	SO ₄	CF	CF	CF	PLI	RR
(g/L)		(mg/L)	(mg/L)	(mg/L)	(mg/L)	(mg/L)	(Fe)	(Mn)	(SO_4)		(%)
1	1.8	3,500	192	459	0.23	5,600	45.9	0.05	14	3.18	66.67
2	1.8	3,190	486	405	0.24	5,783	40.5	0.05	14.46	3.08	83.33
3	1.7	2,592	595	252	0.25	5,093	25.2	0.05	12.73	2.52	83.33
4	3.2	2,424	724	162	0.25	4,797	16.2	0.05	11.99	2.13	83.33
5	3.3	2,219	192	87	0.27	3,991	8.7	0.05	9.98	1.63	66.67
6	3.3	2,017	202	28	0.26	2,560	2.8	0.05	6.4	0.96	66.67
7	3.6	1,975	188	22	0.26	2,450	2.2	0.05	6.12	0.88	50
8	4.2	1,871	178	18	0.21	2,250	1.8	0.04	5.62	0.74	50
9	5.2	1,820	168	13	0.16	2,050	1.3	0.03	5.12	0.58	50
10	8.2	1,725	155	9	0.16	1,750	0.9	0.03	4.38	0.49	16.67

Table 6. CaO Post-treatment diagnostic indices and compliance

These dose index relationships are illustrated in Figure 5 and Figure 6. Figure 5 shows the dose response curve of the Pollution Load Index (PLI), highlighting the progressive reduction with increasing CaO dose. Figure 6 presents the Residual Risk (RR), confirming that while compliance improves markedly, the persistence of sulfate keeps RR above zero.

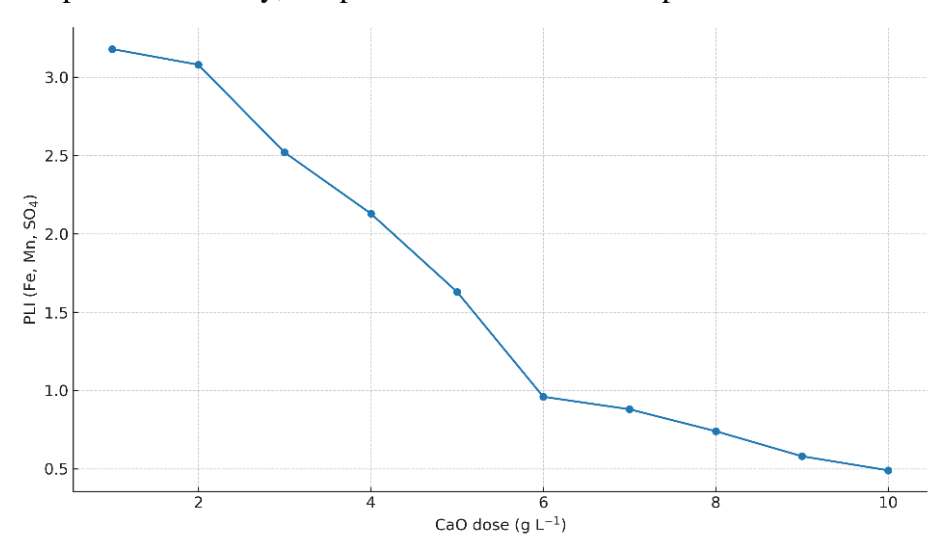


Figure 5. Pollution Load Index (PLI) of CaO

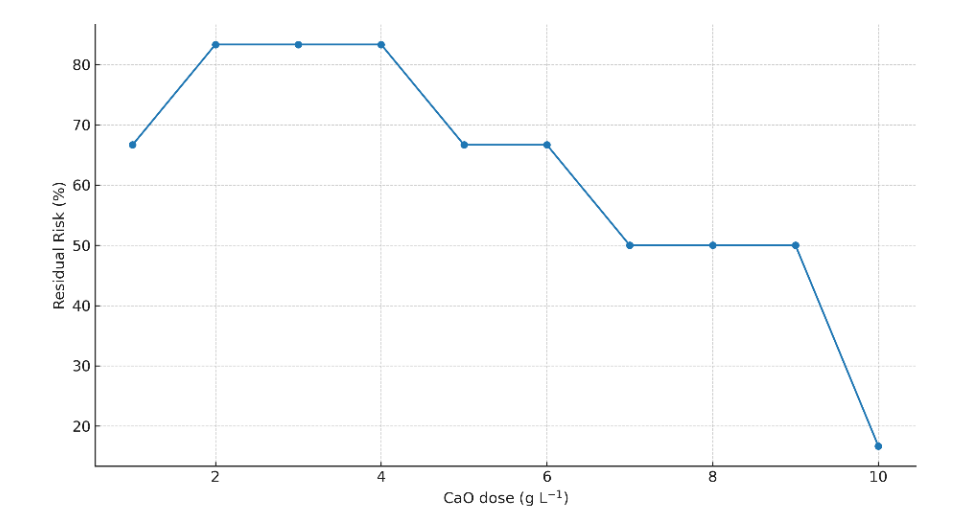


Figure 6. Residual Risk (RR) of CaO

Solids management and polishing need

Neutralization creates suspended solids, so the post-treatment line needs a polishing step to remove these solids and ensure metal compliance. Currently, the ponds offer only 884 m³ of effective storage with a design inflow of about 0.0256 m³/s, which results in a nominal detention time of about 9.6 hours (HRT = V/Q). This is far less than the 84 hours needed for proper settling and sludge management.

To address this issue, we suggest a three-zone rectangular cell (Fig. 7) with a depth of 2.5 m and dimensions that provide a total volume of around 10,125 m³. With the same design flow, the residence time increases to about 110 hours. This meets the polishing goal and offers extra room for sludge buildup between draw-offs. The three-zone design includes internal baffles to reduce short-circuiting.

Operationally, the staged volume can handle the solids produced from CaO-driven Fe/Mn removal and allows time for floc densification and settling. Sludge will be periodically removed from the floors of Zones 2 and 3 and sent to the handling area. The long-HRT setup decreases how often desludging must occur and helps maintain effluent quality despite short-term changes in influent chemistry or flow. Overall, the enlarged 10,125 m³ design matches hydraulics with neutralization chemistry, turning bench-scale dose–response improvements into consistent post-treatment water quality.

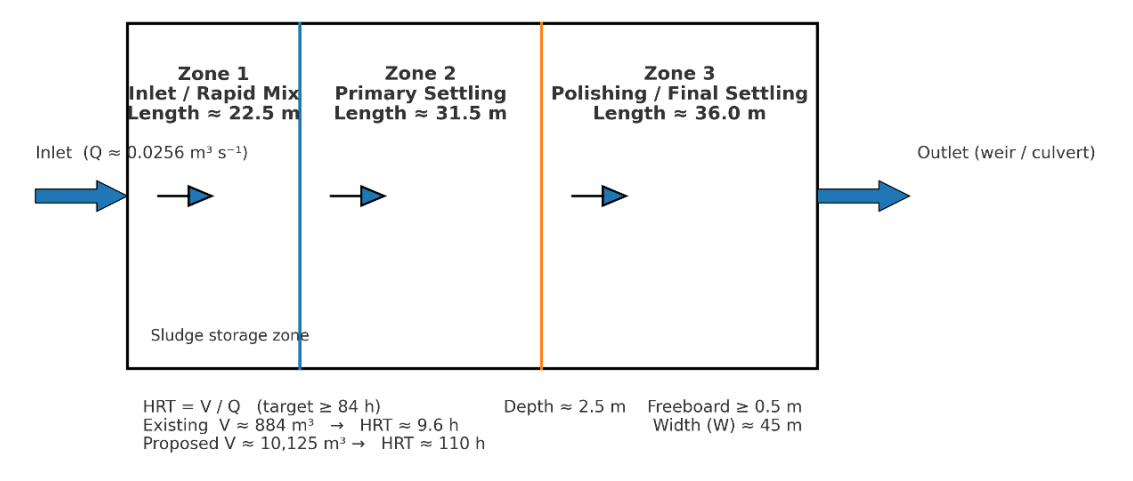


Figure 7. Settling-pond schematic for post-treatment polishing

Implications for instrumentation and design

From an instrumentation perspective, the workflow connects traceable measurements, such as replicated bench tests and standard methods, with clear processing steps like threshold classification, CF-PLI, and RR. This setup allows operators to set dose targets from PLI(dose) and confirm regulatory pass or fail using RR. Meanwhile, HRT sizing offers a hydraulic envelope for TSS polishing. In practice, dosing should be limited to Zone 1, which includes the inlet and rapid mix, to prevent re-suspension. Zones 2 and 3 serve as primary and final settling areas (Fig. 7). The overall result is a consistent pathway from formation evidence to controlled instrument points and important design goals.

Limitations and next steps

Bench tests simulate mixing and contact. At scale, we verify kinetics, especially for Mn, and confirm sludge production and handling under site flows. Seasonal changes and storm events can alter the effective HRT, so we evaluate the polishing step over a ± 20 to 30% range around the design inflow. Since sulfate is the primary compliance issue, possible improvements include staged alkalinity or additional polishing aimed at reducing anions.

CONCLUSION

This study achieved its three stated objectives. First, the IGHRA workflow successfully linked rock formation evidence with the expected behavior of water quality, showing that sulfide-rich and weakly buffered lithologies explain the acidity and metal loads in drainage waters. Second, replicated bench-scale experiments demonstrated that CaO is highly effective in restoring pH and removing Fe and Mn, while CaCO₃ is kinetically limited at low pH and therefore unsuitable as a primary reagent. Third, the performance of both reagents was expressed in terms of diagnostic (CF, PLI) and compliance (RR) indices. For CaO, the PLI decreased from 3.18 at 1 g/L to below 1.0 at doses of 6 g/L and above, and the RR declined from 66.67% to 16.67%, indicating substantial but not complete risk reduction due to the persistence of sulfate. In contrast, CaCO₃ showed limited neutralization under low pH conditions, confirming its role only as a supplementary reagent rather than the main neutralizer. These quantified indices, combined with regulatory thresholds, provide transparent decision points for dosing. Finally, the hydraulic residence time (HRT) framework translated the need for polishing into a design target: expanding the pond volume to 10,125 m³ yields 110 hours of detention time, compared to the current 9.6 hours, ensuring solids removal and performance stabilization.

Overall, the IGHRA approach turns formation evidence, water quality data, and replicated treatment experiments into reproducible indices and design metrics, providing operators and regulators with a clear basis for AMD risk reduction and compliance.

REFERENCES

- Jiao, Y., Zhang, C., Su, P., Tang, Y., Huang, Z., & Ma, T. (2023). A review of acid mine drainage: Formation mechanism, treatment technology, typical engineering cases and resource utilization. *Process Safety and Environmental Protection*, *170*, 1240–1260.
- Kefeni, K. K., Msagati, T. A. M., & Mamba, B. B. (2017). Acid mine drainage: Prevention, treatment options, and resource recovery: A review. *Journal of Cleaner Production*, 151, 475–493.
- 3 Abfertiawan, M. S., Gautama, R. S., Kusuma, S. B., & Notosiswoyo, S. (2016). Hydrology simulation of Ukud river in lati coal mine. *Evergreen*, 3(1), 21–31.
- 4 Gwira, H. A., Osae, R., Abasiya, C., Peasah, M. Y., Owusu, F., Loh, S. K., Kojo, A., Aidoo, P., & Agyare, E. A. (2024). Hydrogeochemistry and human health risk assessment of heavy metal pollution of groundwater in Tarkwa, a mining community in Ghana. *Environmental Advances*,

- 17(June), 100565.
- 5 Czajkowski, M., Meade, N., Seroa da Motta, R., Ortiz, R. A., Welsh, M., & Blanc, G. C. (2023). Estimating environmental and cultural/heritage damages of a tailings dam failure: The case of the Fundão dam in Brazil. *Journal of Environmental Economics and Management*, 121(July).
- Hakanson, L. (1980). An ecological risk index for aquatic pollution control.a sedimentological approach. *Water Research*, *14*(8), 975–1001.
- 7 Tomlinson, D. L., Wilson, J. G., Harris, C. R., & Jeffrey, D. W. (1980). Problems in the assessment of heavy-metal levels in estuaries and the formation of a pollution index. *Helgoländer Meeresuntersuchungen*, 33(1–4), 566–575.
- 8 Government Regulation No. 22 of 2021 on Environmental Protection and Management. Jakarta (ID): Government of Indonesia; 2021. Indonesian.
- 9 Canadian Council of Ministers of the Environment (CCME). Canadian water quality guidelines for the protection of aquatic life: CCME Water Quality Index, User's Manual 2017 Update. In: Canadian environmental quality guidelines, 1999. Winnipeg: Canadian Council of Ministers of the Environment; 2017.
- Drinking Water Inspectorate. (2018, August). *DWI Compliance Risk Index (CRI): Definition*. London: Drinking Water Inspectorate.
- 11 Chidiac, S., El Najjar, P., Ouaini, N., El Rayess, Y., & El Azzi, D. (2023). A comprehensive review of water quality indices (WQIs): history, models, attempts and perspectives. In *Reviews in Environmental Science and Biotechnology* (Vol. 22, Issue 2). Springer Netherlands.
- 12 Akpan, L., Tse, A. C., Dumbari Giadom, F., & Adamu, C. I. (2021). Chemical Characteristics of Discharges from Two Derelict Coal Mine Sites in Enugu Nigeria: Implication for Pollution and Acid Mine Drainage. *Journal of Mining and Environment (JME)*, *12*(1), 89–111.
- Ushakova, E., Menshikova, E., Blinov, S., Osovetsky, B., & Belkin, P. (2022). Environmental Assessment Impact of Acid Mine Drainage from Kizel Coal Basin on the Kosva Bay of the Kama Reservoir (Perm Krai, Russia). *Water 2022, Vol. 14, Page 727, 14*(5), 727.
- 14 Marove, C. A., Sotozono, R., Tangviroon, P., Tabelin, C. B., & Igarashi, T. (2022). Assessment of soil, sediment and water contaminations around open-pit coal mines in Moatize, Tete province, Mozambique. *Environmental Advances*, 8, 100215.
- Elghali, A., Benzaazoua, M., Taha, Y., Amar, H., Ait-khouia, Y., Bouzahzah, H., & Hakkou, R. (2023). Prediction of acid mine drainage: Where we are. *Earth-Science Reviews*, *241*, 104421.
- Syaputra, R., Kusuma, G. J., & Badhurahman, A. (2023). Prediction of Potential Acid Mine Drainage Formation in High Sulfidation Epithermal Deposit using Geochemical and Mineralogy Approaches | EKSPLORIUM. *EKSPLORIUM*, 44(1), 33–40.
- Andini, D. E., & Gautama, R. S. (2019). Prediction Potential Acid Mine Drainage of Epithermal High Sulfidation Deposits using Static Test. *IOP Conference Series: Earth and Environmental Science*, 353(1), 012023.
- National Standardization Agency of Indonesia. (2017). *Indonesian National Standard (SNI)* 8995:2021 Methods for sampling water for physical and chemical testing. Indonesian National Standard, 1–27.
- 19 Brăhaiţa, I. D., Pop, I. C., Baciu, C., Mihăiescu, R., Modoi, C., Popita, G., & Truţă, R. M. (2017). The efficiency of limestone in neutralizing acid mine drainage A laboratory study. *Carpathian Journal of Earth and Environmental Sciences*, 12(2), 347–356.
- Skousen, J. G., Ziemkiewicz, P. F., & McDonald, L. M. (2019). Acid mine drainage formation, control and treatment: Approaches and strategies. *The Extractive Industries and Society*, 6(1), 241–249.
- 21 Masindi, V., Osman, M. S., & Shingwenyana, R. (2019). Valorization of acid mine drainage (AMD): A simplified approach to reclaim drinking water and synthesize valuable minerals-Pilot study. *Journal of Environmental Chemical Engineering*, 7(3).
- Nguegang, B., & Ambushe, A. A. (2024). Insight into the chemical and biochemical mechanisms governing inorganic contaminants removal by selective precipitation and neutralization in acid mine drainage treatment using MgO: A comparative study. *Journal of Water Process Engineering*, 59 (August 2023), 104924.
- Government of the Republic of Indonesia. (2007). *Law of the Republic of Indonesia Number 24 of 2007 on Disaster Management*. State Gazette of the Republic of Indonesia Year 2007 Number

66.

- Government of the Republic of Indonesia. (2025). Government Regulation of the Republic of Indonesia Number 26 of 2025 on Environmental Protection and Management Planning. State Gazette of the Republic of Indonesia Year 2025 Number 96; Supplement to the State Gazette of the Republic of Indonesia Number 7113.
- 25 RoyChowdhury, A., Sarkar, D., & Datta, R. (2015). Remediation of Acid Mine Drainage-Impacted Water. *Current Pollution Reports*, 1(3), 131–141.
- 26 Cheong, Y. W., Cho, D. W., Yim, G. J., Park, H. S., Kim, S. J., & Lee, J. H. (2022). Geochemical Assessment of Gypsum Scale Formation in the Hydrated Lime Neutralization Facility of the Daedeok Mine, South Korea. *Minerals*, 12(5), 1–10.
- Offeddu, F. G., Cama, J., Soler, J. M., Dávila, G., McDowell, A., Craciunescu, T., & Tiseanu, I. (2015). Processes affecting the efficiency of limestone in passive treatments for AMD: Column experiments. *Journal of Environmental Chemical Engineering*, *3*(1), 304–316.
- 28 Ministry of Energy and Mineral Resources of the Republic of Indonesia. (2018). Decree of the Minister of Energy and Mineral Resources of the Republic of Indonesia Number 1827 K/30/MEM/2018 on Guidelines for the Implementation of Good Mining Engineering Principles.